J Comp Physiol B (2010) 180:953–965
DOI 10.1007/s00360-010-0469-7

ORIGINAL PAPER

Acquisition of Ca^{2+} and HCO_3^-/CO_3^{2-} for shell formation in embryos of the common pond snail *Lymnaea stagnalis*

Sue C. Ebanks · Michael J. O'Donnell · Martin Grosell

Received: 31 August 2009 / Revised: 9 March 2010 / Accepted: 11 March 2010 / Published online: 2 April 2010

Abstract Embryos of the freshwater common pond snail *Lymnaea stagnalis* develop to hatch within 10 days under control conditions (22°C, Miami-Dade tap water) and this development is impaired by removal of ambient calcium. In contrast, embryos did not exhibit dependence upon an ambient HCO_3^-/CO_3^{2-} source, developing and hatching in HCO_3^-/CO_3^{2-}-free water at rates comparable to controls. Post-metamorphic, shell-laying embryos exhibited a significant saturation-type calcium uptake as a function of increasing ambient calcium concentration. However, changes in ambient bicarbonate concentration did not influence calcium or apparent titratable alkalinity uptake. There was a distinct shift from no significant flux in pre-metamorphic embryos to net uptake of calcium in post-metamorphic stages as indicated by an increased uptake from the micro-environment surrounding the egg mass and increased net uptake in 24-h, whole egg mass flux measurements. Furthermore, HCO_3^-/CO_3^{2-} acquisition as measured by titratable alkalinity flux is at least partially attributable to an endogenous carbonate source that is associated with acid extrusion. Thus, calcium requirements for embryonic shell formation are met via uptake but HCO_3^-/CO_3^{2-}, which is also necessary for shell formation is acquired in part from endogenous sources with no detectable correlation to ambient HCO_3^-/CO_3^{2-} availability.

Keywords Calcium uptake kinetics · Carbonate · Development · Freshwater · Calcification · Snail metamorphosis

Communicated by I.D. Hume.

S. C. Ebanks (✉) · M. Grosell
Division of Marine Biology and Fisheries,
Rosenstiel School of Marine and Atmospheric Science,
University of Miami, 4600 Rickenbacker Causeway,
Miami, FL 33149, USA
e-mail: sebanks@rsmas.miami.edu

M. J. O'Donnell
Department of Biology, McMaster University,
1280 Main Street West, Hamilton, ON L8S 4K1, Canada

Introduction

The freshwater common pond snail *Lymnaea stagnalis* produces a sessile gelatinous egg capsule (*tunica capsulis*) containing embryos that have a developmental period of approximately 10 days at 22°C. The embryos are contained in prolate spheroidal eggs that are embedded in a gelatinous matrix (*tunica interna*). Features of these egg masses have been previously described in great detail (Bayne 1968; Plesch et al. 1971; Morrill 1982) and we have conformed to the morphological nomenclature used by Plesch et al. (1971) for our purposes here. These embryos metamorphose by approximately day five post-oviposition to produce hippo stage, shell-bearing individuals that will be fully developed snails upon hatching (Morrill 1982). Direct development during the embryonic stage requires that the embryos be provided with sufficient maternally derived elemental substrate for shell formation and/or have the capacity to acquire the necessary ions from the ion-poor freshwater. Early histological and histochemical studies of the egg masses of various species of *Lymnaea* indicate that the embryo is bathed in perivitelline fluid (Bayne 1968; Plesch et al. 1971) that is bound by a double-membrane egg capsule (*membrana interna* and *externa*, Fig. 1A, Plesch et al. 1971). The egg capsules are connected by thin strings embedded in the *tunica interna* (gelatinous matrix) and this complex of up to nearly 100 eggs is bound by a

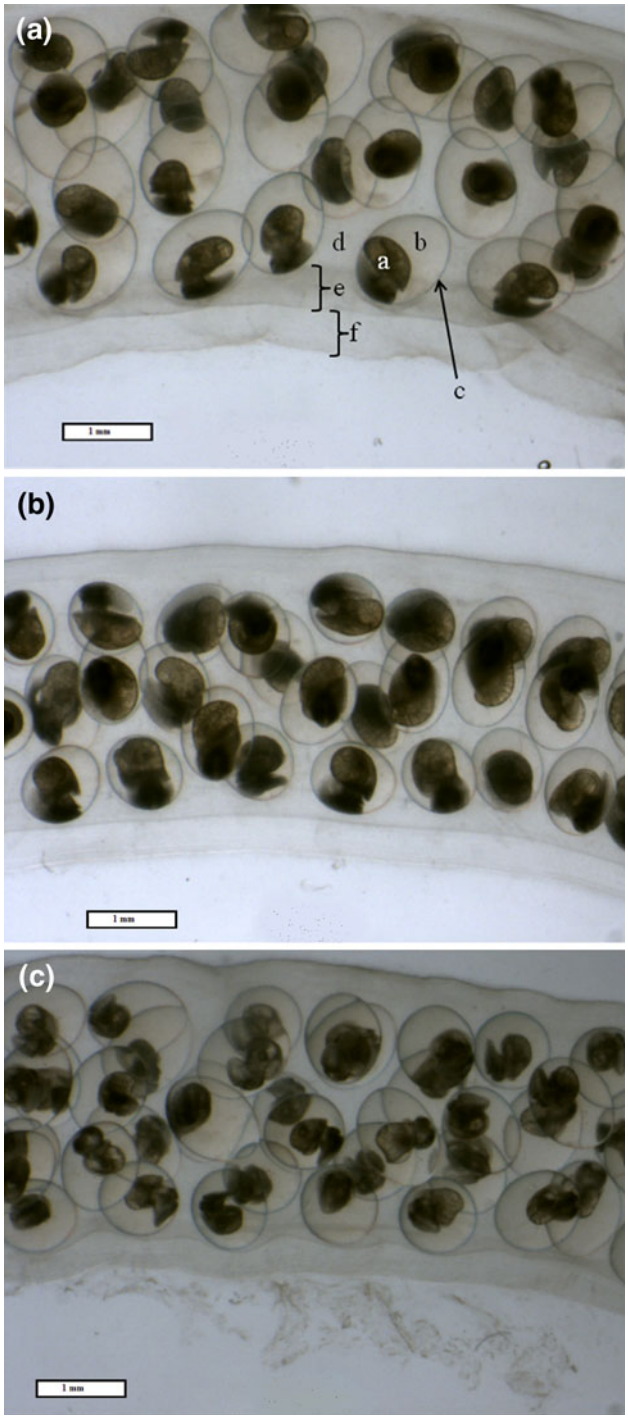

Fig. 1 Day 10 images from a time course of embryonic development of the freshwater common pond snail *L. stagnalis* under control (**a** dechlorinated MDTW, 310 µmol l^{-1} Ca^{2+} and 680 µmol l^{-1} HCO_3^-), nominally HCO_3^--free (**b** 310 µmol l^{-1} Ca^{2+} and 7.5 µmol l^{-1} HCO_3^-), and nominally Ca^{2+}-free (**c** 3 µmol l^{-1} Ca^{2+} and 680 µmol l^{-1} HCO_3^-) conditions. Eggs were placed in the media within 24 h post-oviposition and maintained for the duration of the development with daily water replacement. Morphological characters are identified in **a** (*a*, embryo; *b*, perivitelline fluid; *c*, egg capsule (*membrana interna* and *membrana externa*); *d*, *tunica interna*; *e*, double-layer outer membrane, i.e., *tunica capsulis*; *f*, *Pallium gelatinosum*). *Scale bar* 1 mm

membrane composed mostly of protein and polysaccharides, a double-layered *tunica capsulis*, and usually a *pallium gelatinosum* that is nearly histochemically neutral but usually contains eosinophils, a type of parasite repellant (Plesch et al. 1971). In fact, Bayne (1968) found that proteins are abundant in the egg capsule of this species and in particular in the perivitelline fluids, polysaccharides are present in all layers of the egg mass with neutral ones abundant in perivitelline fluids, and acid mucopolysaccharides are common in the *tunica capsulis*.

In addition to carbohydrates and proteins (Bayne 1968; Plesch et al. 1971; Taylor 1973), snail egg masses have been found to contain maternal stores of shell-forming and other ions in concentrations exceeding that in surrounding waters (Taylor 1973). Using excised eggs with pre-gastrula embryos, Beadle (1969a) studied *L. stagnalis* and found mean calculated perivitelline fluid volume for *L. stagnalis* to be 0.70 mm^3. In his study, the capsular membrane was found to be more permeable to water than ions. In a series of experiments using excised egg capsules that were exposed to either a large sugar (raffinose), solutes of large molecular weight polyethylene glycols (m.w. 500–600 or 3,000), or standard lake water; Beadle (1969a) found that molecules of approximately m.w. 600 could move across the capsular membrane in both directions. Furthermore, an intact gelatinous matrix and outer envelope retarded inward diffusion of raffinose but did not prevent it. Beadle (1969a) also determined that the undifferentiated pre-gastrula embryo could maintain itself in lake water for more than 24 h suggesting that it is capable of actively regulating its salt and water levels. This agrees with later findings by Taylor (1977) who reported that ion uptake and water excretion systems are developed in the earliest cleavage stages in *L. stagnalis* to cope with the problems of osmotic and ionic regulation. Compared to another pulmonate snail examined in the Beadle (1969a) study, *Biomphalaria sudanica*, the gelatinous matrix that surrounds the eggs is thicker in the egg mass of *L. stagnalis* and thus provides a greater buffer between the embryo and the ambient environment considering that the egg capsule provides no significant barrier to the diffusion of water and ions (Beadle 1969a).

In a related study, Beadle (1969b) focused on the Na^+ requirements of developing *B. sudanica* and found that active Na^+ uptake occurred during development, increasing embryonic Na^+ content to seven times that of pre-blastula stage levels. Additionally, and pertinent to our study, he found that the embryos developed normally under reduced [Na^+] of 1/7 normal levels (standard lake water: 0.56 meq l^{-1} Na^+), but total ion reduction to 1/10 of normal resulted in the onset of water balance disruption. This suggests that *B. sudanica* can tolerate a wide range of [Na^+] and possibly other cations with no effect on

embryonic snail development when varied individually. Lastly, Taylor (1977) determined that the exchangeable Ca^{+} content of the embryos increases by five orders of magnitude (1.3 pmol to 130 nmol) over the period from the blastula stage through hatching, clearly demonstrating Ca^{2+} absorption from the egg mass and/or the water.

Considering the ion requirements for calcification, and the ability of *L. stagnalis* embryos to complete direct development in freshwater conditions in a relatively short period of time, we sought to determine whether our target species is provided with adequate quantities of shell-forming ions via maternal stores or actively extract the necessary inorganic ions from ambient waters. Thus, our objectives were to determine [Ca^{2+}] in the perivitelline fluid and gelatinous matrix encasing the eggs over the course of development to determine whether there are significant fluctuations, particularly when comparing pre- and post-metamorphic stages of development. Additionally, we measured fluxes of shell-forming Ca^{2+} ions on the microscale and whole egg mass scale to determine whether egg masses of *L. stagnalis* acquire the necessary Ca^{2+} from environmental sources or are provided with them as maternal stores within the egg mass. Based on preliminary findings it became essential to also determine whether HCO_3^{-}/CO_3^{2-} sources were from exogenous sources or endogenously produced in egg masses containing post-metamorphic embryos as suggested in early respiratory studies on these embryos by Baldwin (1935) and as proposed and modeled by Greenaway (1971a) in adults of this species.

Materials and methods

Animals

Egg masses of the common pond snail *L. stagnalis* were collected in 24-h intervals from mass cultures with the day of collection considered day zero post-oviposition, for age determination. Embryos were incubated at room temperature (20–22°C) in aerated, dechlorinated Miami-Dade County tap water (Grosell et al. 2007). Prior to flux experiments, the egg masses were weighed (g), measured (mm), and viability was determined. Egg masses with less than 80% development were excluded from experiments and analyses.

Visual characterization of development

Specimens were examined using a dissecting microscope fitted with a Nikon Coolpix digital camera with Q-Capture software to preserve a time course of images from day zero through hatching and to determine developmental stages under standardized conditions. Additionally this system was utilized to catalogue developmental differences, particularly ovum/shell length among embryos raised in control (Miami-Dade tap water), nominally Ca^{2+}-free (measured 3 μmol l^{-1} Ca^{2+}), and nominally HCO_3^{-}-free (measured 7.5 μmol l^{-1} HCO_3^{-}) media (Table 1).

Voltage and Ca^{2+}-selective microelectrodes

Microelectrodes, used for recordings of voltage across the *tunica capsulis* or the *membrana interna* and *externa*, were pulled from filamented 1.5 mm diameter borosilicate capillary glass (WPI, Sarasota, FL, USA). The microelectrodes were filled with 3 mol l^{-1} KCl and had tip resistances of approximately 30 MΩ. Ca^{2+}-selective microelectrodes used to measure Ca^{2+} concentration in the *tunica interna* and perivitelline fluid were pulled from unfilamented 1.5 mm borosilicate capillary glass (A-M systems, Carlsborg, WA, USA), silanized by exposure to the vapors of dimethyldichlorosilane at 200°C and stored over silac gel until use. Microelectrodes were backfilled with 100 mmol l^{-1} $CaCl_2$ and tip-filled with a 300–500 μm column of Ca^{2+} ionophore I, cocktail A (Fluka, Buchs, Switzerland). Microelectrodes were mounted on micromanipulators (Marzhauser MM33, Fine Science Tools, North Vancouver, BC, Canada) and observed through a dissecting microscope (Wild-Leitz, Heidelberg, Germany).

For measurement of Ca^{2+} concentration in the *tunica interna* of day 2 egg masses, it was necessary to cut two slits, each approximately 300 μm long, in the *tunica capsulis* using the tip of a 25 gauge syringe needle. This

Table 1 Nominal chemical concentrations for artificial waters

Miami-Dade tap water (μmol l^{-1})	Ca^{2+}-free media (μmol l^{-1})	HCO_3^{-}-free media (μmol l^{-1})
1100 Na^{+}	650 $NaHCO_3$	1000 NaCl
1030 Cl^{-}	500 NaCl	120 $MgSO_4{\cdot}7H_2O$
680 HCO_3^{-}	50 $KHCO_3$	40 KCl
310 Ca^{2+}	120 $MgSO_4{\cdot}7H_2O$	310 $C_{12}H_{22}CaO_{14}$
40 K^{+}		
120 Mg^{2+}		
110 SO_4^{2-}		

Values for Miami-Dade tap water from Grosell et al. 2007

incision was necessary because the outer integument of the *tunica capsulis* was too rigid to pierce with the microelectrode without compromising the electrode. The outer integument became increasingly fluidic over the course of development, making the pre-incision necessary only for day 2 measurements. For older egg masses it was feasible to advance the microelectrodes directly across the *tunica capsulis* and into the *tunica interna*. A voltage electrode was then inserted through one slit and advanced 1–2 mm into the *tunica interna* and the Ca^{2+}-selective microelectrode was inserted through the second slit. The voltage detected by the voltage microelectrode was subtracted from that detected by the Ca^{2+}-selective microelectrode, yielding a signal proportional to Ca^{2+} concentration. Voltage and Ca^{2+}-selective microelectrodes were connected through a high impedance ($>10^{14}$ Ω) electrometer (pH/ion Amp, A-M systems, Carlsborg, WA, USA) to a PC-based data acquisitions and analysis system (PowerLab 4/25, AD Instruments, Colorado Springs, CO, USA) running CHART software (AD Instruments).

Calcium concentration ($[Ca^{2+}]_{med}$) in the bathing medium (i.e. artificial Miami-Dade water) was calculated as:

$$[Ca^{2+}]_{med} = [Ca^{2+}]_{cal} 10^{(\Delta V/S)}$$

where $[Ca^{2+}]_{cal}$ is the calcium concentration in a calibration solution (0.1, 1 or 10 mmol l^{-1} Ca^{2+}), ΔV is the voltage difference recorded from the calcium electrode between the medium and the same calibration solution, and S is the slope of the microelectrode for a tenfold change in calcium concentration. Although ion-selective microelectrodes measure ion activity and not concentration, data can be expressed in terms of concentrations if it is assumed that the ion activity coefficient is the same in calibration and experimental solutions. Expression of data in units of concentrations aids comparison of Ca^{2+} microelectrode data with techniques such as atomic absorption spectrophotometry, which measures Ca^{2+} concentration. Concentrations can be converted to activities by multiplying by the activity coefficient (0.81 for Miami-Dade tap water). It is important to point out that activity measurements may underestimate calcium concentrations in the *tunica interna* and the perivitelline fluid. This is because polyvalent anions will lower the activity coefficient, relative to the surrounding water, and because some Ca^{2+} is likely bound to macromolecules and not readily diffusible, as demonstrated by Taylor (1973).

Calcium concentration ($[Ca^{2+}]_{ti}$) in the *tunica interna* (i.e. gelatinous matrix) was then calculated as:

$$[Ca^{2+}]_{ti} = [Ca^{2+}]_{med} 10^{(\Delta V/S)}$$

where ΔV is the voltage difference recorded from the calcium electrode between the matrix and the bathing medium.

For measurement of net electrochemical potential, no slits were made in the *tunica capsulis* and voltage and Ca^{2+}-selective microelectrodes were advanced through the *tunica capsulis* and both voltage and Ca^{2+}-selective microelectrodes were referenced to a bath electrode constructed from a 1.5 mm glass capillary filled with 3 mol l^{-1} KCl in 3% agar and connected through a Ag/AgCl half cell to the ground input of the amplifier. This procedure sometimes caused the ionophore column to be pushed back from the tip of the Ca^{2+}-selective microelectrode, requiring replacement of the Ca^{2+}-selective microelectrode. The net electrochemical potential ($\Delta\mu^{tc}_{Ca}/F$) in mV for Ca^{2+} across the *tunica capsulis* was calculated as:

$$\begin{aligned}\Delta\mu^{tc}_{Ca}/F &= RT/F \ln\left([Ca^{2+}]_{ti}/[Ca^{2+}]_{med}\right) + zV_{tc} \\ &= 58 \log\left([Ca^{2+}]_{ti}/[Ca^{2+}]_{med}\right) + zV_{tc}\end{aligned}$$

where R is the gas constant, T is the temperature (degrees Kelvin), z is the valence, and V_{tc} is the voltage difference across the *tunica capsulis*. A positive value indicates that the concentration of Ca^{2+} in the *tunica interna* is above that expected on the basis of electrochemical equilibrium, and that passive efflux across the *tunica capsulis* and into the bathing medium is therefore favored.

For measurements of calcium concentration in the perivitelline fluid and for calculations of net electrochemical potential across the *membrana interna* and *externa*, voltage- and Ca^{2+}-selective microelectrodes were advanced through the membranes and into the perivitelline fluid. The calcium concentration in the perivitelline fluid ($[Ca^{2+}]_{PVF}$) was calculated as

$$[Ca^{2+}]_{PVF} = [Ca^{2+}]_{med} 10^{(\Delta V/S)}$$

The net electrochemical potential across the *membrana interna* and *externa* ($\Delta\mu^{mi\&me}_{Ca}/F$) was calculated as:

$$\Delta\mu^{mi\&me}_{Ca}/F = 58 \log\left([Ca^{2+}]_{PVF}/[Ca^{2+}]_{med}\right) + zV_{mi\&me}$$

where $V_{mi\&me}$ is the voltage difference between the perivitelline fluid and the bathing medium for isolated eggs (i.e. across the *membrana interna* and *externa* together). Dividing $\Delta\mu$ by the Faraday converts the units to mV (Dawson and Liu 2008). A positive value indicates that the concentration of Ca^{2+} in the perivitelline fluid is above that expected on the basis of electrochemical equilibrium, and that passive efflux across the *membrana interna* and *externa* and into the bathing medium is therefore favored.

Time course of Ca^{2+}, titratable alkalinity, and ammonia fluxes—whole egg masses

To evaluate whether the embryos were developing fully from maternal stores or were extracting necessary Ca^{2+} and HCO_3^-/CO_3^{2-} from the water over the course of development, eight egg masses were selected from mass cultures, scored, and placed in individual flux chambers that contained 20 ml of Miami-Dade tap water. Daily 10 ml initial stock and final water samples were collected for each egg mass. Daily net Ca^{2+} flux was determined using the difference in $[Ca^{2+}]$ between the initial and final waters following the 24-h flux as measured by flame atomic absorption spectrophotometry (Varian SpectrAA220, Mulgrave, Victoria, Australia), mass of egg mass (g), and elapsed time (h). Daily net titratable alkalinity flux was calculated from the change in titratable alkalinity from the initial and final flux media samples as determined via double-endpoint titration, mass of egg mass (g), and elapsed time (h). The double-endpoint titration, rather than a standard titration method, was used to determine titratable alkalinity because the double-endpoint titration method is insensitive to non-bicarbonate/carbonate buffering in the media. This technique has been suggested (Hills 1973) and since modified (Wilson et al. 1996) and used successfully for this type of titratable alkalinity determination (Wilson et al. 1996; Grosell et al. 1999). In experiments with low volume:biomass ratios the potential for release of organic material with buffer capacity exists which could lead to erroneous conclusions based on single-endpoint titrations. For the double-endpoint titration procedure, which avoids this problem, a 5 ml flux media sample with 5 ml of pH electrode-stabilization media (450 mmol l^{-1} NaCl) were gassed with N_2 for 30 min after which starting pH was noted. Using a Gilmont micro-burette syringe filled with 0.02 N HCl, the sample was titrated down to pH 3.8 and 15 min was allowed for CO_2 degassing. Sample pH was then returned to the original pH value using a second Gilmont micro-burette syringe filled with 0.02 N NaOH while continuously gassed. Using the difference in the amount of acid and base necessary to titrate to 3.800 and the start pH, HCO_3^-/CO_3^{2-} titratable alkalinity equivalents were determined. To evaluate whether the changes in titratable alkalinity were attributable to ammonia flux, we determined ammonia excretion rates over the course of development by calculating total ammonia concentration in initial and final water samples from the 24-h flux. Total ammonia was assessed using a modified colorimetric ammonia assay (Verdouw et al. 1978) in which ammonia was reacted with salicylate and hypochlorite to form a blue indophenol in a sodium nitroprusside-catalyzed reaction. The assay was measured on a micro-plate reader (Molecular Devices ThermoMax, Sunnyvale, CA, USA) at 640 nm. Final values for Ca^{2+} and titratable alkalinity net flux as well as total ammonia excretion were presented as μmol g^{-1} h^{-1}.

Time course of Ca^{2+} fluxes-microscale measurements using the scanning ion electrode technique

Transport of Ca^{2+} into or out of egg masses produces gradients in $[Ca^{2+}]$ in the unstirred layer adjacent to the surface of the tissue. These gradients can be calculated from the voltages recorded by a Ca^{2+}-selective microelectrode moved between two points within the unstirred layer. Calcium flux can then be calculated from the concentration gradients using Fick's law, as described below. Measurement of fluxes in this way is the basis of the scanning ion electrode technique (SIET), which allows fluxes to be repeatedly measured in near real-time at sites along the length of an egg mass. Extensive descriptions of the use of SIET are reported in Rheault and O'Donnell (2001, 2004) and Donini and O'Donnell (2005).

SIET measurements were made using hardware from Applicable Electronics (Forestdale, MA, USA) and automated scanning electrode technique (ASET) software (version 2.0) from Science Wares Inc. (East Falmouth, MA, USA). Egg masses were placed in 35 mm diameter petri dishes filled with 5 ml of artificial Miami-Dade water. Reference electrodes were made from 10 cm lengths of 1.5 mm borosilicate glass capillaries that were bent at a 45° angle, 1–2 cm from the end, to facilitate placement in the sample dish. Capillaries were filled with boiling 3 mol l^{-1} KCl in 3% agar and connected to the ground input of the Applicable Electronics amplifier through an Ag/AgCl half cell.

Ca^{2+}-selective microelectrodes for use with SIET were calibrated in 0.1, 1, and 10 mmol l^{-1} Ca^{2+}. All scans were performed in artificial Miami-Dade water with a Ca^{2+} concentration of 310 μmol l^{-1}. The Ca^{2+}-selective microelectrode was initially placed 5–10 μm from the surface of the egg mass. The microelectrode was then moved a further 50 μm away, perpendicular to the egg mass surface. The "wait" and "sample" periods at each limit of the 50 μm excursion distance were 4.5 and 0.5 s, respectively. Voltage differences across this excursion distance were measured three times at each of the 5–18 sites along each egg mass and scans of the same sites were repeated four or more times over a 1-h period. Voltage differences were corrected for electrode drift measured at a reference site 10–20 mm away from the egg mass. Voltage differences (ΔV) were converted to the corresponding $[Ca^{2+}]$ difference by the following equation (Donini and O'Donnell 2005):

$$\Delta C = C_B \times 10^{(\Delta V/S)} - C_B$$

where ΔC is the $[Ca^{2+}]$ difference between the two limits of the excursion distance (μmol cm^{-3}), C_B is the background $[Ca^{2+}]$ in the bathing medium, ΔV is the voltage difference (mV); and S is the slope of the electrode between 0.1 and 1 mmol l^{-1} Ca^{2+}.

Concentration differences were used to determine the Ca^{2+} flux using Fick's law of diffusion:

$$J_{Ca} = D_{Ca}(\Delta C/\Delta X)$$

where J_{Ca} is the net flux in μmol cm^{-2} s^{-1}, D_{Ca} is the diffusion coefficient of Ca^{2+} (1.19×10^{-5} cm^2 s^{-1}), ΔC is the Ca^{2+} concentration difference (μmol cm^{-3}) and ΔX is the excursion distance between the two points (cm).

Ca^{2+} and HCO_3^-/CO_3^{2-} kinetics

For Ca^{2+} uptake kinetics experiments, day 7 egg masses were incubated for 24 h in 20 ml of media with nominal ion concentrations approximating that of Miami-Dade tap water except for Ca^{2+}, which was adjusted to nominal concentrations of 10, 20, 60, 90, 100, 200, 600, or 900 μmol l^{-1} Ca^{2+} using $CaCl_2$ (Sigma–Aldrich). Egg masses were dip-rinsed in appropriate flux media prior to the start of the flux. For determination of fluxes, 10 ml of initial media stock and 10 ml of final media from flux chambers were collected for each treatment. Calcium and titratable alkalinity net flux were determined for each $[Ca^{2+}]$ as described above in the time course section and presented as μmol g^{-1} h^{-1}.

For HCO_3^- kinetics experiments, $[Ca^{2+}]$ was maintained at 310 μmol l^{-1} and $[HCO_3^-]$ was adjusted to either 200, 400, 800, or 1,200 μmol l^{-1} HCO_3^- with choline bicarbonate (Sigma–Aldrich, [2-hydroxyethyl] trimethylammonium, $C_5H_{14}NO{\cdot}HCO_3$). Both Ca^{2+} net flux and titratable alkalinity net flux were determined for each $[HCO_3^-]$. Ammonia fluxes were not included here due to the nearly undetectable concentrations measured during the time course experiments. Egg masses and flux procedures were handled in the same manner as described above for time course and Ca^{2+} kinetics experiments.

Fluxes in HCO_3^-/CO_3^{2-}-free HEPES-buffered media

Day 7 egg masses were scored and dip-rinsed then placed in individual chambers with 20 ml of flux media that contained either 680 μmol l^{-1} HCO_3^-, which is comparable to Miami-Dade tap water, or HCO_3^-/CO_3^{2-}-free HEPES-buffered media (1.5 mmol l^{-1} each HEPES-free H^+ and HEPES-Na^+ salt; Sigma–Aldrich) with all other ions maintained at concentrations comparable to Miami-Dade tap water. This concentration of HEPES provided for adequate buffering under bicarbonate-free conditions while still allowing for measurements of changes in apparent titratable alkalinity (Grosell and Taylor 2007). Egg masses were incubated for 24 h. Then 15 ml of the initial and final media samples were taken and analyzed for $[Ca^{2+}]$, titratable alkalinity, and total ammonia. Net Ca^{2+} flux was determined as described above. Net titratable alkalinity flux was calculated from results of single-endpoint titrations on initial and final media samples as outlined in Grosell and Taylor (2007). In the absence of HCO_3^-/CO_3^{2-}, changes in apparent titratable alkalinity would be a result of H^+ excretion and its effects (i.e. NH_4^+ trapping). Therefore, it was not necessary to complete double-endpoint titrations as in the HCO_3^-/CO_3^{2-}-buffered solutions. For the single-endpoint procedure, aliquots of 10 ml were collected and gassed continuously in 50 ml Falcon tubes with N_2 for 30 min prior to and during the titration to insure the absence of CO_2. pH was noted following the initial 30 min gassing and then the 10 ml sample was titrated using a Gilmont micro-burette syringe filled with 0.02 N HCl down to pH 7.0 noting the pH and amount of 0.02 N HCl added at the final pH and for no less than three points along the titration curve. Linearity was conserved down to pH 7.0 but was lost below that value thus $[H^+]$ values below pH 7.0 were not used in the H^+ excretion calculation. Initial and final samples were titrated on the same pH electrode and with the same burette. All curves were fit by non-linear regression analysis and only those curves for which $R^2 > 0.95$ were included. The titratable alkalinity net flux (=acid excretion) was calculated using the difference between the H^+ added to reach the known pH of 7.0 for both the initial and final flux media, the mass of the egg mass (g), and the elapsed flux time (h). Total ammonia excretion was determined as described above.

Statistical analyses

Uptake kinetic constants, apparent affinity (k_m) and capacity (V_{max}), were determined assuming Michaelis–Menten saturation kinetics and using the non-linear regression function in SigmaPlot for Windows version 11.00. Comparisons among experimental groups were completed using an ANOVA with pairwise comparisons where appropriate following the Holm–Sidak method after an evaluation for whether the data sets were normally distributed with the Shapiro–Wilk test. All values are mean ± SEM and statements of statistical difference were reserved for a P value < 0.05.

Results

Developmental observations

Embryos grew from an ovum diameter of 100 μm at day 2 to a shell length of 800 μM at day 10 under control conditions and were enclosed in egg capsules that were

approximately 1 × 1.25 mm. Eggs were firmly nested in the *tunica interna* of the egg mass and the entire mass was encased in the *tunica capsulis*, which was approximately 300–400 μm thick. The outermost layer, the *pallium gelatinosum*, was approximately 100–200 μm thick. There was no apparent loss in egg viability observed for those egg masses incubated in nominally HCO_3^-/CO_3^{2-}-free artificial Miami-Dade tap water relative to controls; however, those raised in nominally Ca^{2+}-free media exhibited growth retardation relative to controls in all treated egg masses (e.g. Figs. 1, 2). Control embryos developed to hatching within 10–12 days post-oviposition, and metamorphosis to the hippo stage occurred at approximately day 5. Reduced aquatic availability of Ca^{2+} resulted in reduced growth rates and longer times to hatch. However, embryos incubated in HCO_3^--free water exhibited faster growth rates relative to controls and Ca^{2+}-free conditions around the time of metamorphosis (day 4 and day 7, Fig. 2). Embryos raised in Ca^{2+}-free water were significantly smaller than controls beginning with day 8 and showed no growth after day 8 (Fig. 2). Those incubated in HCO_3^--free media developed to approximately the same size by the end of embryonic development as controls but those in Ca^{2+}-free media developed much less consistently and most individuals in this treatment group did not hatch or reach pre-hatch size within 15–18 days.

Endogenous Ca^{2+} sources

Considering the disparity in developmental rates among varying ambient water conditions it was necessary to evaluate Ca^{2+} availability in the perivitelline fluid bathing the embryos and in the gelatinous matrix (*tunica interna*) that surrounded the eggs. This was accomplished with the use of Ca^{2+}-selective microelectrodes. Calcium concentration in the gelatinous matrix holding eggs of pre-metamorphic embryos was 3–4 times greater than that of the bathing media (Fig. 3). Furthermore, $[Ca^{2+}]_{PVF}$ was 5–7 times that of the bathing media (Fig. 4).

The visible onset of shell formation, an indicator of metamorphosis, at approximately day 5, was concurrent

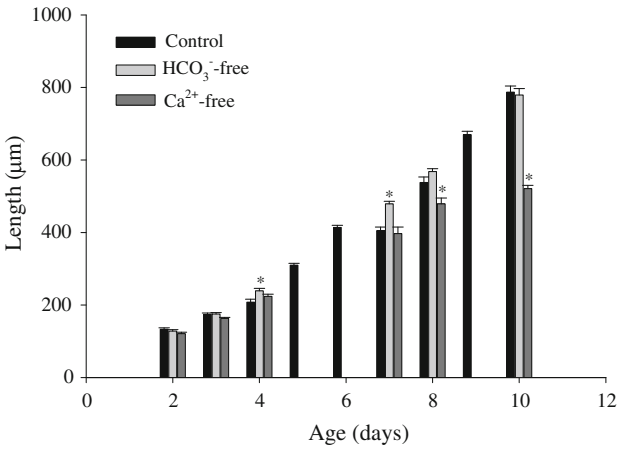

Fig. 2 Pre-metamorphic ovum diameter and post-metamorphic shell lengths of embryos of *L. stagnalis* (μm ± SEM) in control (dechlorinated MDTW; 310 μmol l^{-1} Ca^{2+} and 680 μmol l^{-1} HCO_3^-), nominally HCO_3^--free (310 μmol l^{-1} Ca^{2+} and 7.5 μmol l^{-1} HCO_3^-), and nominally Ca^{2+}-free (3 μmol l^{-1} Ca^{2+} and 680 μmol l^{-1} HCO_3^-) media. $N = 10$ ova or embryos for each measurement. *Significant difference from controls of the same age

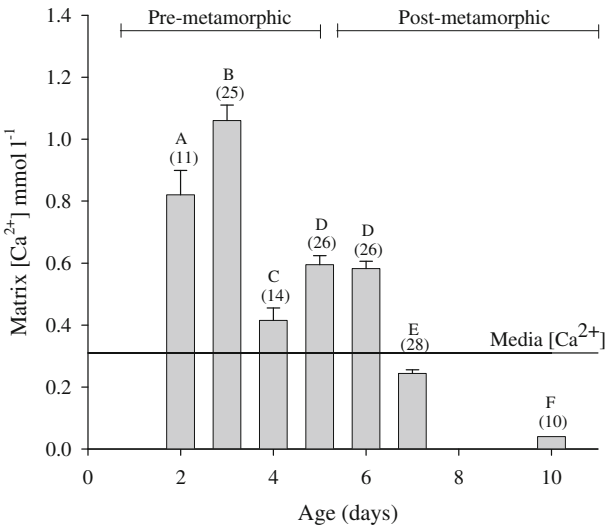

Fig. 3 Mean concentrations of Ca^{2+} in the *tunica interna* (mmol l^{-1} ± SEM) as measured on day 2–10 with Ca^{2+}-selective microelectrodes. Greater than 80% egg viability was observed in all cases. *Numbers in parentheses* indicates sample size for indicated time point. Developmental stages with the *same letter* notation are not significantly different. Water $[Ca^{2+}] = 0.31$ mmol l^{-1}

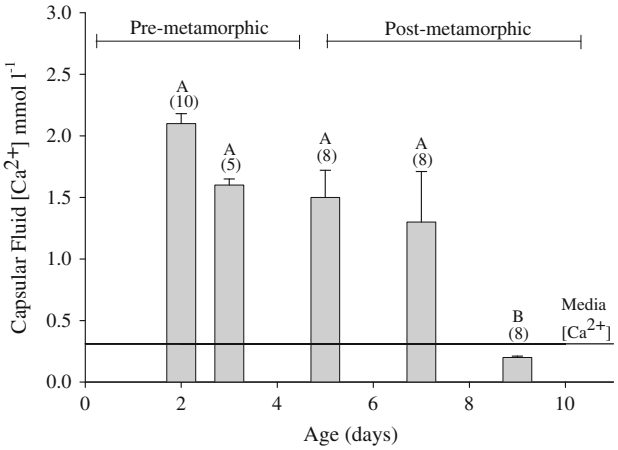

Fig. 4 Mean concentration of Ca^{2+} in perivitelline fluid (mmol l^{-1} ± SEM) as measured on day 2–9 with Ca^{2+}-selective microelectrodes. *Numbers in parentheses* indicate sample size for indicated time point. Developmental stages with the *same letter* notation are not significantly different. Water $[Ca^{2+}] = 0.31$ mmol l^{-1}

with significantly decreased [Ca^{2+}] in the *tunica interna* of post-metamorphic egg masses to levels below pre-metamorphic concentrations. Also, perivitelline fluid from post-metamorphic (day 7 and 9) eggs had significantly lower [Ca^{2+}] than eggs containing pre-metamorphic embryos (Fig. 4). Results from the aforementioned experiments indicated a need to consider the likelihood of important interactions between the egg mass and its contents with the surrounding environment, particularly in post-metamorphic stages.

Exogenous Ca^{2+} sources

Using Ca^{2+}-selective and voltage microelectrodes for measurements of [Ca^{2+}] and transmembrane voltage difference, respectively, we were able to quantify the net electrochemical potential ($\Delta\mu_{Ca}/F$) across these barriers in peri- and post-metamorphic stages. Day 7 $\Delta\mu_{Ca}/F$ (−19.7 mV) and ΔV (−9.2 ± 0.60 mV) values were negative across the *tunica capsulis* membrane. After emergence of the embryos from the egg capsules on day 10, but prior to their emergence from the egg mass, mean $\Delta\mu_{Ca}/F$ became more negative (−51.0 mV) with no significant change in transmembrane voltage difference (−8.7 ± 1.11 mV, inside negative). For excised eggs, mean $\Delta\mu_{Ca}/F$ across the *membrana interna* and *externa* was more negative on day 9 (−26.4 mV) relative to peri-metamorphic values (day 5, −3.7 mV); however, the voltage difference across these membranes became less negative over the same time period (day 5: −21.4 ± 0.92 mV, day 9: −9.1 ± 0.77 mV).

Measurements of 24-h whole egg mass Ca^{2+} net flux with daily water replacement indicated net uptake of Ca^{2+} and titratable alkalinity, but only after metamorphosis and with no significant change in ammonia excretion (Fig. 5). A time course of near-daily microscale flux measurements indicated a shift from nearly no Ca^{2+} flux during pre-metamorphic stages to net uptake on day 5. Net uptake rates increased and continued through post-metamorphosis within the unstirred boundary layer (Fig. 6). Calcium uptake rates, which were calculated from the unstirred boundary layer concentration gradients, peaked around day 8–9. Site-specific measurements of several post-metamorphic egg masses indicated that the uptake was uniform across the surface of the egg mass (data not shown). When exposed to a range of [Ca^{2+}], actively transporting, day 7 egg masses exhibited net uptake rates across the range in a significant Michaelis–Menten, saturation-type relationship (Fig. 7a).

Flux of acid–base equivalents

Titratable alkalinity net flux varied over the range of ambient [Ca^{2+}] in a saturation-like pattern particularly at

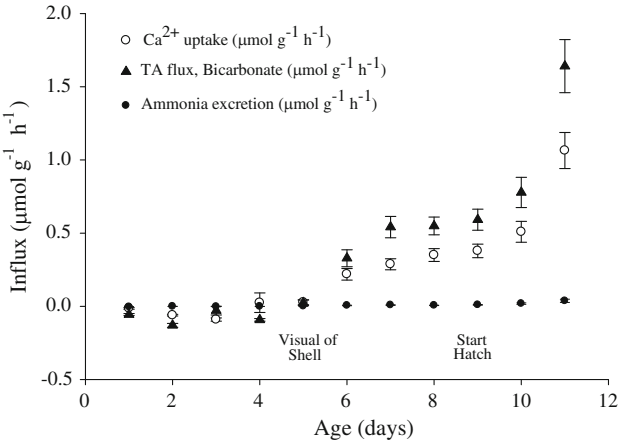

Fig. 5 Daily net Ca^{2+}, titratable alkalinity (TA), and total ammonia fluxes (μmol g^{-1} h^{-1} ± SEM) for 11 subsequent 24-h periods for developing egg masses. $N = 8$ egg masses analyzed for each data point as measured in Miami-Dade Tap Water [Ca^{2+}] = 506 ± 3 μmol l^{-1}

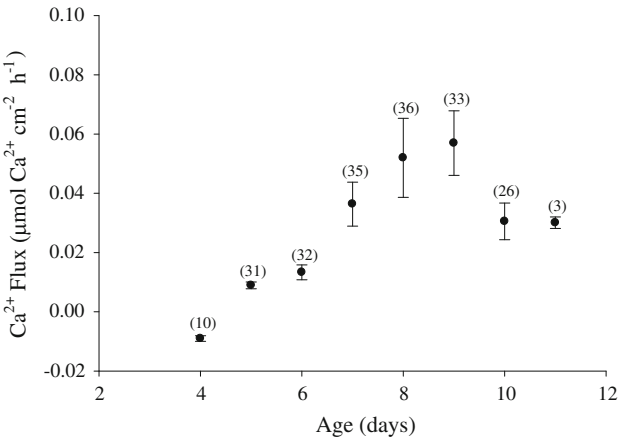

Fig. 6 SIET measurement of microscale Ca^{2+} flux over development (μmol cm^{-2} h^{-1} ± SEM) for *L. stagnalis* egg masses. *Numbers in parentheses* indicate sample size for indicated time point. Water [Ca^{2+}] = 310 μmol l^{-1}

concentrations ≤170 μmol l^{-1} Ca^{2+}, with saturation occurring above 170 μmol l^{-1} Ca^{2+} (Fig. 7b). The manipulation of ambient water [HCO_3^-] over the nominal range of 200–1,200 μmol l^{-1} HCO_3^- resulted in no significant changes in net Ca^{2+} transport (Fig. 8a) and no correlation with net titratable alkalinity transport rates (Fig 8b). However, there was a significant effect on Ca^{2+} net flux, titratable alkalinity net flux, and ammonia excretion for egg masses under HCO_3^--free HEPES-buffered conditions. Net Ca^{2+} uptake was significantly greater under HCO_3^--free, HEPES-buffered conditions relative to controls (Fig. 9a) while net titratable alkalinity flux was approximately 1/3 that of the controls (Fig. 9b). Lastly, under HCO_3^--free, HEPES-buffered conditions, ammonia

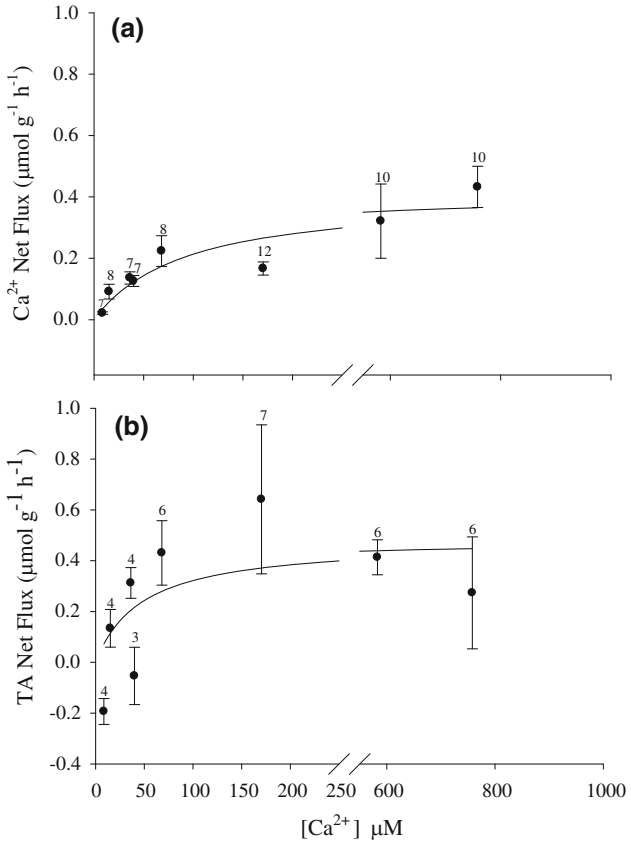

Fig. 7 Mean net Ca^{2+} (**a**) and titratable alkalinity (**b**) fluxes (µmol g^{-1} h^{-1} ± SEM) as a function of ambient [Ca^{2+}] for egg masses of the pond snail *L. stagnalis*. Values are for day 7 egg masses that were fluxed for 24 h. Regression line is a Michaelis–Menten curve (Net Ca^{2+}: $k_m = 91 \pm 41.5$ µmol l^{-1} Ca^{2+}, $V_{max} = 0.4 \pm 0.06$ µmol g^{-1} h^{-1}, $R^2 = 0.84$, $P < 0.002$). There was no significant relationship between [Ca^{2+}] and TA net flux ($P > 0.05$); however the curve is the best fit trace assuming Michaelis–Menten saturation kinetics. Sample size is indicated for respective [Ca^{2+}] above each data point

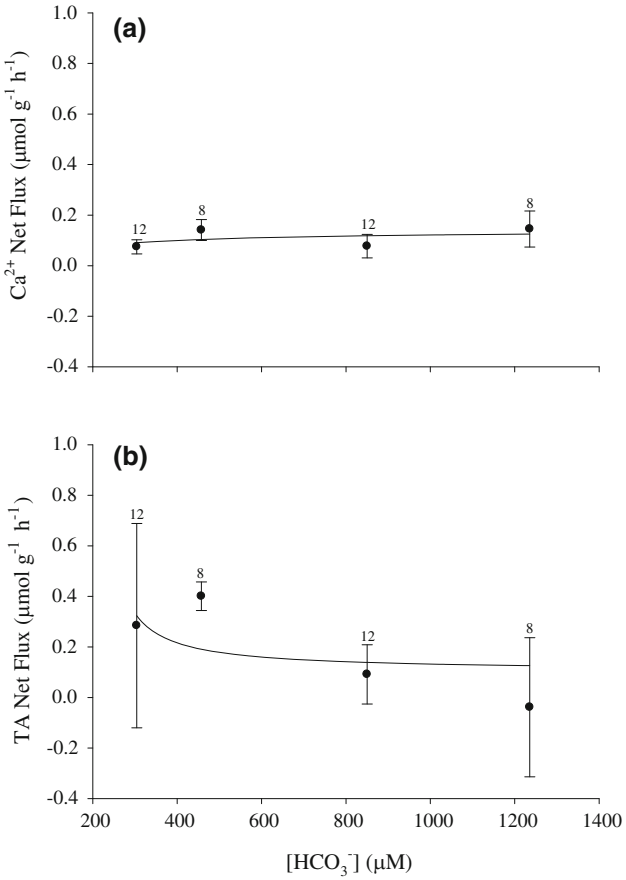

Fig. 8 Mean net Ca^{2+} (**a**) and titratable alkalinity (**b**) fluxes (µmol g^{-1} h^{-1} ± SEM) as a function of ambient [HCO_3^-] for egg masses of the pond snail *L. stagnalis*. Values are for day 7 egg masses that were fluxed for 24 h. There was no apparent relationship between Ca^{2+} or TA net flux and [HCO_3^-]. Sample size is indicated for respective [HCO_3^-] above each data point

excretion rates were significantly greater than control values with rates nearly 2 1/2 times that in controls (Fig. 9c).

Discussion

Developing embryos of *L. stagnalis* showed visible dependency on environmental Ca^{2+} sources after depletion of maternal stores in the form of reduced growth rates (Figs. 3, 4), but no apparent dependence on exogenous HCO_3^-/CO_3^{2-} sources (Fig. 2). We also observed a distinct difference in the structural integrity of the egg mass membrane (i.e., resistant to penetration during early development but more permeable in post-metamorphic stages) and significant differences in the Ca^{2+} content and $\Delta\mu_{Ca}/F$ over the course of development, but particularly during peri- and post-metamorphic stages. Thus, it was important to consider interactions between the contents of the egg mass and the surrounding environment that may facilitate the process of embryonic acquisition of shell-forming ions.

The saturation-type kinetics that we observed in the post-metamorphic embryos of *L. stagnalis* were remarkably similar to those reported by Greenaway (1971b) in adults of the species. Greenaway calculated a half-saturation point of 300 µmol Ca^{2+} l^{-1} and determined that the uptake pathway reached the maximum of 0.5 µmol g^{-1} h^{-1} at 1,000–1,500 µmol Ca^{2+} l^{-1}. That maximum value was comparable to the maximum of 0.4 µmol g^{-1} h^{-1} at above 600 µmol Ca^{2+} that we found here. However, our half-saturation value (91 µmol Ca^{2+} l^{-1}) was nearly 1/3 of his calculated value. This may be due to the difference in developmental stage (embryonic versus adult), difference in pre-experimental [Ca^{2+}], or other parameters.

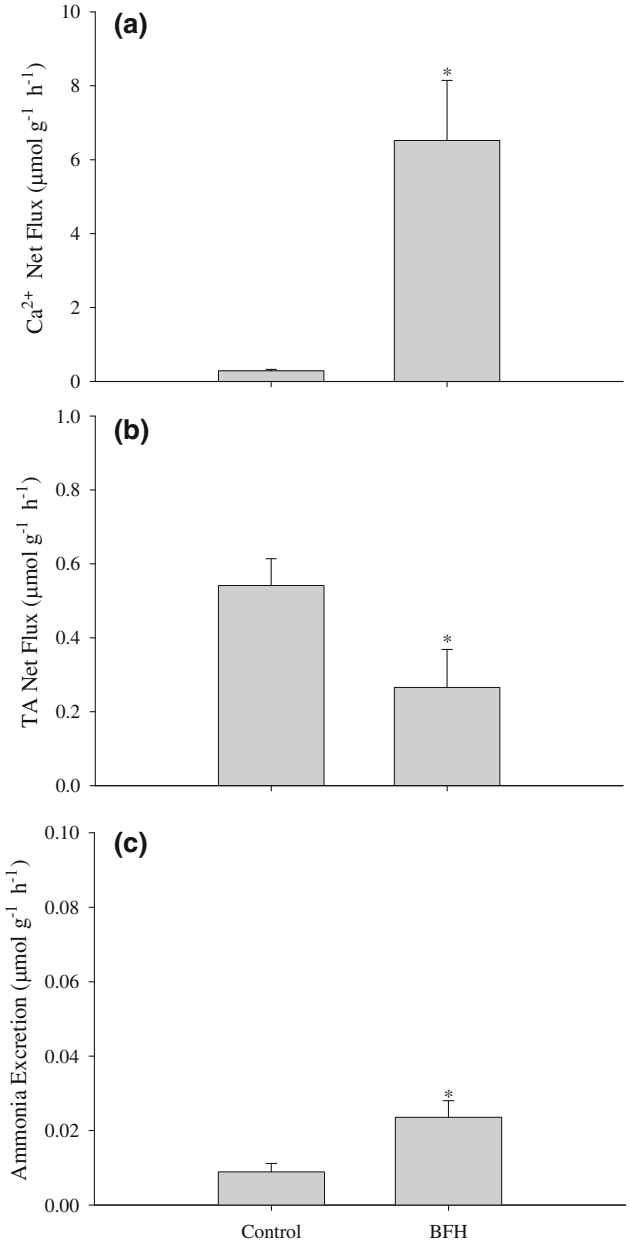

Fig. 9 Mean net Ca^{2+} uptake (**a**), titratable alkalinity uptake (**b**), and ammonia excretion (**c**) rates (μmol g^{-1} h^{-1} ± SEM) under control (bicarbonate-buffered, 680 μmol l^{-1} HCO_3^-) and nominally HCO_3^--free (HEPES-buffered (BFH), 7.5 μmol l^{-1} HCO_3^-, 3 mmol l^{-1} HEPES) media conditions. Values are for day 7 egg masses that were fluxed for 24 h. $N = 8$ for controls and $N = 7$ for treatment. *Significantly different from bicarbonate-buffered ($P < 0.05$)

Over the course of development, we noted changes in the penetrability of the integument of the *tunica capsulis*, and fluctuations in [Ca^{2+}] in the perivitelline fluid consistent with the presence and use of maternal stores during pre-metamorphic stages. The earliest studies on various vertebrate eggs including *Raja*, *Triton*, *Bufo*, and salmonid species in freshwater environments indicated changes in their permeability to water and ions during development from impermeability to semi-permeability (Gray 1920; Krogh and Ussing 1937; Krogh et al. 1939). The changes in the degree of permeability to water and/or ions were attributed to changes in the protoplasmic membrane (limiting layer) coupled with embryonic activation of osmoregulatory mechanisms. At the egg and embryonic level of development, Krogh (1965) clearly stated that there was no reason to distinguish between vertebrates and invertebrates in freshwater because the problem of preserving maternal ionic stores against the strong outward gradient is universal particularly until the mechanisms for osmoregulation have developed and become active. In preliminary whole egg mass experiments, we observed net uptake of Ca^{2+} from incubation media with developing *L. stagnalis* egg masses but not when the embryos were dead (data not shown). In later time course experiments we found that egg masses incubated in nominally Ca^{2+}-free and HCO_3^--free media were affected by lack of Ca^{2+} availability in the incubation media but not by HCO_3^--free conditions, which suggests that there is an alternative HCO_3^-/CO_3^{2-} source for shell formation. The increased Ca^{2+} uptake in HCO_3^--free HEPES-buffered conditions points to a likely connection between Ca^{2+} uptake and apparent HCO_3^-/CO_3^{2-} acquisition under depleted HCO_3^-, yet buffered, conditions.

The presence of internal Ca^{2+} stores may explain why when embryos had essentially no exogenous Ca^{2+} sources available they still developed shell but exhibited retarded growth relative to controls. We measured 2 mmol Ca^{2+} l^{-1} in perivitelline fluid of in situ eggs containing pre-metamorphic embryos (Fig. 4). This is less but on the same order of magnitude as the 6–7.5 mmol Ca^{2+} l^{-1} (12–15 meq Ca^{2+} l^{-1}) measured by Taylor (1973). There are procedural and possibly population differences to take into consideration between the two studies. Within his study there were greater differences in [Ca^{2+}] between perivitelline fluids of eggs from different egg masses compared to those taken from the same egg mass. This suggests that [Ca^{2+}] in perivitelline fluids of eggs from different snails may differ and account for part of the difference between our observations and those of Taylor (1973). Also around the onset of shell formation, when internal Ca^{2+} stores were depleted, substantial Ca^{2+} uptake from the water occurred as evident from both net flux measurements on whole egg masses and microscale measurements whereas there was no significant net movement of either shell-forming ion in pre-metamorphic stages (Fig. 5). Nonetheless, Taylor (1973) calculated that Ca^{2+} activity in the perivitelline fluid was 4.8 mequiv l^{-1} (i.e., 2.4 mmol l^{-1}), in good agreement with our value of 2 mmol l^{-1} in pre-metamorphic embryos. The difference between activity and concentration in the perivitelline fluid may reflect interactions of Ca^{2+} with polyvalent anions and binding of Ca^{2+} by macromolecules. As a result, the Ca reserves in the *tunica interna* and PVF

are probably considerably larger than indicated by measurements of Ca^{2+} based on microelectrodes, which measure Ca^{2+} activity.

Measurements of perivitelline fluid using a Ca^{2+}-selective microelectrode revealed that there were significant Ca^{2+} stores in the perivitelline fluid (5–7 times that of the incubation media, Fig. 4) and gelatinous matrix (3–4 times incubation media, Fig. 3) surrounding the eggs of the egg masses during early developmental stages but that these stores apparently become depleted around the time of shell formation. During metamorphosis or at least by day 7, an inside negative $\Delta\mu_{Ca}/F$ exists across the membranes separating the embryo from the aquatic environment. This potential was more strongly negative with emergence of the embryos from the egg capsules on day 10. This change in $\Delta\mu_{Ca}/F$ was attributed to decreased $[Ca^{2+}]$ in the perivitelline fluid and *tunica interna*. After metamorphosis, but prior to emergence of embryos from the egg mass, mean $\Delta\mu_{Ca}/F$ across the *tunica capsulis* became more negative (day 7: −19.7 mV, day 10: −51.0 mV) despite a lack of significant change in transmembrane voltage difference (day 7: -9.2 ± 0.60 mV, day 10: -8.7 ± 1.11 mV). However, the strengthening in $\Delta\mu_{Ca}/F$ from day 7 to day 10 was accompanied by decreased $[Ca^{2+}]$ in the *tunica interna* to 20% of day 7 values (Fig. 3). For excised eggs, mean $\Delta\mu_{Ca}/F$ across the *membrana interna* and *externa* was more negative on day 9 (−26.4 mV) relative to peri-metamorphic values (day 5, −3.7 mV), but the voltage difference across these membranes became less negative over the same time period (day 5: -21.4 ± 0.92 mV, day 9: -9.1 ± 0.77 mV). Thus, the increase in $\Delta\mu_{Ca}/F$ was likely due to the decrease in $[Ca^{2+}]$ to 13% of day 5 values (Fig. 4). The depletion of maternal stores available for calcification to concentrations below aquatic levels (Figs. 3, 4) thus favors diffusive Ca^{2+} influx in these later stages (i.e. movement of Ca^{2+} down the concentration gradient from the ambient media to the Ca^{2+}-depleted perivitelline fluid).

Considering the aforementioned findings as well as our observations of changes in *tunica capsulis* integrity over the development of the embryos and findings by Beadle (1969a) that *Biomphalaria sudanica* embryos have osmoregulatory capabilities, we propose that around the time of embryonic metamorphosis there is also a concurrent change in the membranes of the egg mass. The altered state may allow for Ca^{2+} diffusion and/or uptake as influenced by Ca^{2+} removal from the perivitelline fluid by the embryo for calcification. Thus, the *tunica interna* and *tunica capsulis* may serve to resist ion efflux during early developmental phases but allow Ca^{2+} uptake during shell formation. Our techniques did not allow us to isolate what role, if any, the limiting membrane, which is located between the *tunica interna* and *tunica capsulis*, plays in this development of permeability.

High calcium accretion of nearly fivefold over the course of development (Taylor 1977) apparently leads to a reduction in $[Ca^{2+}]$ in the *tunica interna* by day 7 (Fig. 3) and perivitelline fluid by at least day 9 (Fig. 4) to concentrations below ambient media. This provides a reasonable explanation for the observed increase in the inside negative $\Delta\mu_{Ca}/F$ over the post-metamorphic stages. One point for further consideration is that reduced $[Ca^{2+}]_{PVF}$ to below water concentrations may allow for less energy consumptive Ca^{2+} uptake. Similar measurements were made by Taylor (1973) on pre-gastrula (pre-metamorphic) stage embryos. Taylor excised pre-gastrula stage (<24 h old) egg capsules from the *tunica interna* and allowed them to equilibrate with experimental media for at least 24 h at 22–25°C. In contrast, the microelectrode measurements reported as part of the present study for post-metamorphic embryos were taken immediately after eggs were excised and completed within 1–2 h.

The concomitant occurrence of several events have lead us to consider that it may not be just the embryo that metamorphoses but that the embryo–egg mass complex transforms over the course of development. Maternal Ca^{2+} reserves provided in the perivitelline fluid apparently decrease over development. This reduction is concurrent with strengthening of inward negative $\Delta\mu_{Ca}/F$ across the membranes between the developing embryo and the aquatic environment. Around this same time, active Ca^{2+} uptake from the surrounding medium also begins. In the SIET measurements, day 7 egg masses exhibited a net Ca^{2+} flux of 0.04 μmol cm^{-2} h^{-1}, which translates to 0.48 μmol g^{-1} h^{-1} for an egg mass 2 cm long and 0.43 cm diameter. This was of the same order of magnitude as the 0.29 μmol g^{-1} h^{-1} that we measured in whole egg mass net Ca^{2+} fluxes. Furthermore, documented accumulation of 0.13 μmol Ca^{2+}/embryo in isolated eggs over the period from the blastula stage through hatching (Taylor 1977) equates to 7.7 μmol Ca^{2+} over the time period for an average egg mass with 59 eggs. The blastula stage occurs during the latter half of day 1 for *L. palustris* embryos maintained at 25°C (Morrill 1982). In whole egg mass fluxes, our embryos, which were maintained at 20–22°C, removed 16.9 μmol Ca^{2+} from flux media over the period of day 2–11. Thus, our flux measurements using microscale and whole egg mass methods produced similar results and were in reasonable agreement with literature values.

Similar trends were expected in titratable alkalinity kinetics as those observed for Ca^{2+} kinetics over a range of ambient bicarbonate and/or $[Ca^{2+}]$. However, considering (1) that embryos developed in HCO_3^-/CO_3^{2-}-free media, (2) the lack of a significant relationship between HCO_3^-/CO_3^{2-} transport and either Ca^{2+} or HCO_3^- availability, and (3) a significant apparent titratable alkalinity flux under HCO_3^--free, HEPES-buffered conditions there is

apparently another source of HCO_3^-/CO_3^{2-} for these post-metamorphic embryos. The likely HCO_3^-/CO_3^{2-} source in *L. stagnalis* is hydration of endogenous, metabolic CO_2. The notion of retaining and using endogenously produced HCO_3^-/CO_3^{2-} for calcification was suggested by Baldwin (1935) following measurements of oxygen consumption and bound CO_2 in *L. stagnalis* embryos. He reported significantly greater O_2 uptake rates with developmental progress. Furthermore, the onset of the formation of true shell, which was labeled as stage II in the study, was concurrent with a spiked increase in CO_2 content and O_2 consumption. In a study on the adults of this species, Greenaway (1971a) proposed a model in which Ca^{2+} was exchanged between the external medium, blood, fresh tissues, and shell compartments. Additionally, H^+ and HCO_3^- that were produced through the hydration of metabolic CO_2 were exchanged for Ca^{2+} from the external medium and used for $CaCO_3$ deposition, respectively. To maintain HCO_3^-/CO_3^{2-} production from CO_2 hydration ($CO_2 + H_2O \rightarrow HCO_3^- + H^+ \rightarrow CO_3^{2-} + H^+$) and allow for continued shell formation, H^+ extrusion is necessary. Indeed, such H^+ extrusion likely accounts for the apparent titratable alkalinity uptake in HCO_3^--free media because net acid excretion would be expressed as apparent base uptake when measuring changes in concentrations of absolute alkalinity equivalents. This suggestion is supported by Taylor (1973), who reported that lowering the pH in the bathing medium from 8.5 to 4.0 reduced the concentration of Ca^{2+} in the perivitelline fluid by up to 85%. We propose that the increase in water $[H^+]$ in the Taylor (1973) study would drastically reduce the capacity to excrete H^+. Cation uptake in freshwater fish (Bury and Wood 1999; Fenwick et al. 1999; Grosell and Wood 2002; Lin and Randall 1991) and in *L. stagnalis* (Ebanks and Grosell 2008) has been linked to an electrochemical gradient that is in part established by excretion of the H^+ from carbonic anhydrase-mediated hydration of respiratory CO_2. Calcium uptake in *Lymnaea* exposed to low ambient pH would likely be impaired, explaining the earlier observations by Taylor (1973) of reduced $[Ca^{2+}]$ in the perivitelline fluid.

Lastly, the observed increase in ammonia excretion and Ca^{2+} uptake under HCO_3^-/CO_3^{2-}-free HEPES-buffered conditions was another indicator of the use of endogenously produced HCO_3^-/CO_3^{2-} in post-metamorphic embryos. Under these conditions the embryos would be forced to rely exclusively on the hydration of CO_2 to produce the necessary HCO_3^-/CO_3^{2-} for shell formation thus producing greater amounts of H^+ to be excreted to the surrounding media in order to maintain acid–base balance and favorable internal conditions for calcification. Increased ammonia excretion, as a result of further acidification of boundary layers and consequent diffusion trapping of NH_3 as NH_4^+, may thereby explain the observations of elevated ammonia excretion in absence of ambient HCO_3^-/CO_3^{2-}. The increased H^+ excretion under HCO_3^-/CO_3^{2-}-free HEPES-buffered conditions would possibly also enhance hyperpolarization of the apical membrane, which would provide a stronger electrochemical gradient leading to the observed increased Ca^{2+} uptake.

Conclusions

Utilizing whole egg mass and microscale analytical techniques, we have confirmed the need for aquatic Ca^{2+} for proper development and timely hatching of embryos of the freshwater common pond snail *Lymnaea stagnalis*. The embryos apparently utilize an endogenous source of HCO_3^-/CO_3^{2-} because they can develop in the absence of ambient HCO_3^-/CO_3^{2-}. Furthermore, increased Ca^{2+} uptake under HCO_3^-/CO_3^{2-}-depleted conditions indicates a connection between Ca^{2+} transport pathways and endogenous HCO_3^-/CO_3^{2-} production and thus H^+ extrusion. Therefore, we propose that while Ca^{2+} requirements for complete embryonic shell formation and development are met via uptake, the necessary HCO_3^-/CO_3^{2-} is acquired in part from endogenous sources, likely via carbonic anhydrase-catalyzed hydration of CO_2 coupled with H^+ extrusion with no significant correlation to ambient HCO_3^-/CO_3^{2-} availability. Lastly, excretion of H^+ from hydration of CO_2 seems to facilitate uptake of Ca^{2+}, a subject of ongoing studies.

Acknowledgments We thank Drs. Lynne Fieber and Michael Schmale of the University of Miami, RSMAS for use of their cameras & microscopes and Andrea Kocmarek and Erin Leonard, M.Sc. of McMaster University for their technical assistance during S. Ebanks' visit to the O'Donnell laboratory. This research was funded in part by the NOAA Educational Partnership Program, Environmental Cooperative Science Center and the RSMAS Marine Science Graduate Student Organization Student Travel Fund.

References

Baldwin E (1935) The energy sources in ontogenesis: VII. The respiratory quotent of developing gastropod eggs. J Exp Biol 12:27–35

Bayne CJ (1968) Histochemical studies on the egg capsules of eight gastropod molluscs. Proc Malacological Soc Lond 38:199–212

Beadle LC (1969a) Salt and water regulation in the embryos of freshwater pulmonate molluscs I. The embryonic environment of *Biomphalaria sudanica* and *Lymnaea stagnalis*. J Exp Biol 50:473–479

Beadle LC (1969b) Salt and water regulation in the embryos of freshwater pulmonate molluscs III. Regulation of water during the development of *Biomphalaria sudanica*. J Exp Biol 50:491–499

Bury NR, Wood CM (1999) Mechanism of branchial apical silver uptake by rainbow trout is via the proton-coupled Na^+ channel. Am J Physiol Regul Integr Comp Physiol 277:R1385–R1391

Dawson DC, Liu X (2008) Osmoregulation: some principles of water and solute transport. In: Evans DH (ed) Osmotic and ionic regulation. CRC Press, Boca Raton, pp 1–36

Donini A, O'Donnell MJ (2005) Analysis of Na^+, Cl^-, K^+, H^+ and NH_4^+ concentration gradients adjacent to the surface of anal papillae of the mosquito *Aedes aegypti*: application of self-referencing ion-selective microelectrodes. J Exp Biol 208:603–610

Ebanks SC, Grosell M (2008) Fluid and osmolyte recovery in the common pond snail *Lymnaea stagnalis* following full-body withdrawal. J Exp Biol 211:327–336

Fenwick JC, Wendelaar Bonga SE, Flik G (1999) In vivo bafilomycin-sensitive Na(+) uptake in young freshwater fish. J Exp Biol 202:3659–3666

Gray J (1920) The relation of the animal cell to electrolytes. J Physiol 53:308–319

Greenaway P (1971a) Calcium regulation in the freshwater mollusc *Limnaea stagnalis* (L.) (Gastropoda: Pulmonata): II. Calcium movements between internal calcium compartments. J Exp Biol 54:609–620

Greenaway P (1971b) Calcium regulation in the freshwater mollusc *Limnaea stagnalis* (L.) (Gastropoda; Pulmonata): I. The effect of internal and external calcium concentration. J Exp Biol 54:199–214

Grosell M, Taylor JR (2007) Intestinal anion exchange in teleost water balance. Comp Biochem and Physiol 148:14–22

Grosell M, Wood CM (2002) Copper uptake across rainbow trout gills: mechanisms of apical entry. J Exp Biol 205:1179–1188

Grosell M, De Boek G, Johannsson O, Wood CM (1999) The effects of silver on intestinal ion and acid-base regulation in the marine teleost fish, *Parophrys vetulus*. Comp Biochem and Physiol C 124:259–270

Grosell M, Blanchard J, Brix KV, Gerdes R (2007) Physiology is pivotal for interactions between salinity and acute copper toxicity to fish and invertebrates. Aquatic Toxicol 84:162–172

Hills AG (1973) Acid–base balance: chemistry, physiology, pathophysiology. The Williams and Wilkins Co., Baltimore

Krogh A (1965) Osmotic regulation in aquatic animals. Dover Publications, New York, pp 170–190

Krogh A, Ussing HH (1937) A note on the permeability of trout eggs to D_2O and H_2O. J Exp Biol 14:35–37

Krogh A, Schmidt-Nielsen K, Zeuthen E (1939) The osmotic behaviour of frogs eggs and young tadpoles. J Comp Physiol A 26:230–238

Lin H, Randall D (1991) Evidence for the presence of an electrogenic proton pump on the trout gill epithelium. J Exp Biol 161:119–134

Morrill JB (1982) Development of the pulmonate gastropod, *Lymnaea*. In: Harrison W, Cowdon RF (eds) Developmental biology of freshwater invertebrates. Alan R. Liss, New York, pp 399–483

Plesch B, de Jong-Brink M, Boer HH (1971) Histological and histochemical observations on the reproductive tract of the hermaphrodite pond snail *Lymnaea stagnalis* (L.). Neth J Zool 21:180–201

Rheault M, O'Donnell MJ (2001) Analysis of K^+ transport in Malpighian tubules of *Drosophila melanogaster*: evidence for spatial and temporal heterogeneity. J Exp Biol 204:2289–2299

Rheault MR, O'Donnell MJ (2004) Organic cation transport by Malpighian tubules of *Drosophila melanogaster*: application of two novel electrophysiological methods. J Exp Biol 207:2173–2184

Taylor HH (1973) The ionic properties of the capsular fluid bathing embryos of *Lymnaea stagnalis* and *Biomphalaria sudanica* (Mollusca: Pulmonata). J Exp Biol 59:543–564

Taylor HH (1977) The ionic and water relations of embryos of *Lymnaea stagnalis*, a freshwater pulmonate mollusc. J Exp Biol 69:143–172

Verdouw H, Van Echteld CJA, Dekkers EMJ (1978) Ammonia determination based on indophenol formation with sodium salicylate. Water Res 12:399–402

Wilson R, Gilmour K, Henry R, Wood C (1996) Intestinal base secretion in the seawater-adapted rainbow trout: a role in acid–base balance? J Exp Biol 199:2331–2343